J. Fluid Mech. (1981), *vol.* 108, *pp.* 345–361
Printed in Great Britain

Nonlinearity of the three-dimensional flow past a flat blunt ship

By GILLES FERNANDEZ†
Ecole Nationale Supérieure de Techniques Avancées,
Equipe de Recherche Associée,
au Centre National de la Recherche Scientifique, Paris

(Received 19 October 1979 and in revised form 5 January 1981)

The nonlinearity of the gravity sea flow past a three-dimensional flat blunt ship with a length-based Froude number of order unity is studied using the method of matched asymptotic expansions. It is shown that the nonlinearity is important in an inner domain near the ship, whereas the flow in the rest of the fluid domain is the solution of a Neumann–Kelvin problem. Two possible inner solutions – a jet and a wave – are obtained and discussed.

1. Introduction

The computation of the wave resistance of ships has been the subject of a voluminous literature since the beginning of the century. But it has not yet received a definitive solution, despite the various mathematical approaches tried recently. One of these, which uses assumption of an ideal fluid, consists of looking for the potential of the flow as the solution of a Neumann–Kelvin problem. According to Brard (1972): 'this problem can be called the Neumann–Kelvin problem, for the boundary condition on the hull is of Neumann type, while the boundary condition on the free surface is that used by Lord Kelvin when, the first of all, he initiated the mathematical researches on ship waves'. A complete derivation of the equations of the Neumann–Kelvin problem can be found in the paper by Newman (1976); the main characteristic of that problem is the linearized free-surface condition, which may be written down in the following dimensionless form:

$$F_L^2 \phi_{xx} + \phi_z = 0 \quad \text{on} \quad z = 0, \tag{1.1}$$

where x and z are respectively the horizontal and vertical co-ordinates moving with the ship, ϕ is the velocity potential, and $F_L^2 = U^2/gL$ with U the speed of the ship, g the gravity and L a characteristic length of the flow, say the ship length. It is this linearization that is the source of much dispute about the Neumann–Kelvin problem.

As Noblesse (1976) pointed out, the linearization of the free surface may be justified by the combination of several conditions. For example, a balance between the bluntness and the speed of the ship can make small the surface disturbance. Supporters of the Neumann–Kelvin model argue that good agreement may be found between the theory and experiments, thus, Chang (1977) and Guével, Delhommeau & Cordonnier (1977) are satisfied with the comparison between their computations and the experimental results they display for submerged or surface-piercing bodies.

† Present address: Service Technique des Constructions et Armes Navales, BA/N, 8 Boulevard Victor – 75015 Paris.

Nevertheless, such arguments do not seem to convince the opponents of the Neumann–Kelvin theory. For instance, Tuck (1977), who declares himself 'a known enemy of the Neumann–Kelvin problem', doubts the validity of the linearization. Such a view can be supported by the results of Dagan & Tulin (1972, hereafter referred to as I), Nichols & Hirt (1975) or Tuck & Vanden-Broeck (1977). An analytical two-dimensional study which provides evidence of the existence of a jet at the forebody is reported in I. But there is a discrepancy between their results and that obtained by the method of the present paper. This is more completely discussed in § 8. The other two papers furnish numerical results showing significant nonlinear phenomena in the vicinity of a surface-piercing body. Nichols & Hirt give a striking description of the transient growth of a three-dimensional jet near an impulsively started box-like body, the length-based Froude number of which is $F_L \simeq 0{\cdot}9$. Tuck & Vanden-Broeck solve numerically the nonlinear problem of a steady two-dimensional flow past a semi-infinite body. At the stern, they present results, for $F_L \simeq 2$,† which make it obvious that the free surface cannot be linearized. At the bow, their method does not apply directly, but they obtain results, for $F_L \simeq 1{\cdot}34$,† which suggest strongly the presence of a jet.

However, the contradiction between the two opinions just given is perhaps not so strong. Indeed, the computed wave resistance is rarely compared to experiments for F_L^2 greater than 0·25 or 0·30. On the contrary, the nonlinear phenomena become quite obvious only for F_L^2 near 1. One might think that the nonlinearity cannot be neglected beyond some critical value of F_L, depending on the bluntness of the body. The present work originates from the need of knowing if the extension of the method of Jami & Lenoir (1978) to the three-dimensional case of a surface-piercing body could be adapted in order to take into account the nonlinear behaviour of the fluid, when necessary. Its purpose is to provide an analytical description of the flow in the region of non-uniformity of the linearized Neumann–Kelvin solution. To this end, with the aid of the matched asymptotic expansions method, it studies a case in which one has to expect an important nonlinearity: that of a blunt ship with F_L of order unity.

The method used could be compared to that applied by Nguyen & Rojdestvenskii (1975) who study an hydroplaning wing in finite water depth. In their problem, there are indeed three characteristic lengths: (i) the wing chord $\tilde{c}$; (ii) the wing span $\tilde{l}$, which is of the same order as the water depth; (iii) the characteristic length of inertia phenomena, say $L = U^2/g$. One can associate to each of them a domain: $\mathscr{D}_{\tilde{c}}$, $\mathscr{D}_{\tilde{l}}$, $\mathscr{D}_L$. The authors choose assumptions such that: $\tilde{l}/L \ll \tilde{c}/\tilde{l} \ll 1$. As a consequence, the gravity does not play any role in $\mathscr{D}_{\tilde{c}}$ nor $\mathscr{D}_{\tilde{l}}$. Besides this, they do not state the problem in $\mathscr{D}_L$; thus $\mathscr{D}_{\tilde{l}}$ is their 'outer' domain and $\mathscr{D}_{\tilde{c}}$ their inner domain in which they point out the presence of a jet.

On the contrary, in the present paper, there are only two characteristic lengths: (i) the ship length L, or equivalently U^2/g since $F_L^2 \simeq 1$, and (ii) the ship draft T, small compared to L, whence two domains. In the inner domain, near the ship water-line, the problem stated is a nonlinear one which is solved analytically. In the rest of the fluid domain (outer domain), the problem is a Neumann–Kelvin one according to Brard's definition; the complete resolution of this problem would imply the use of a

† Here, F_L is based on the length they use to make the co-ordinates dimensionless, which is consistent with the scope of the present paper.

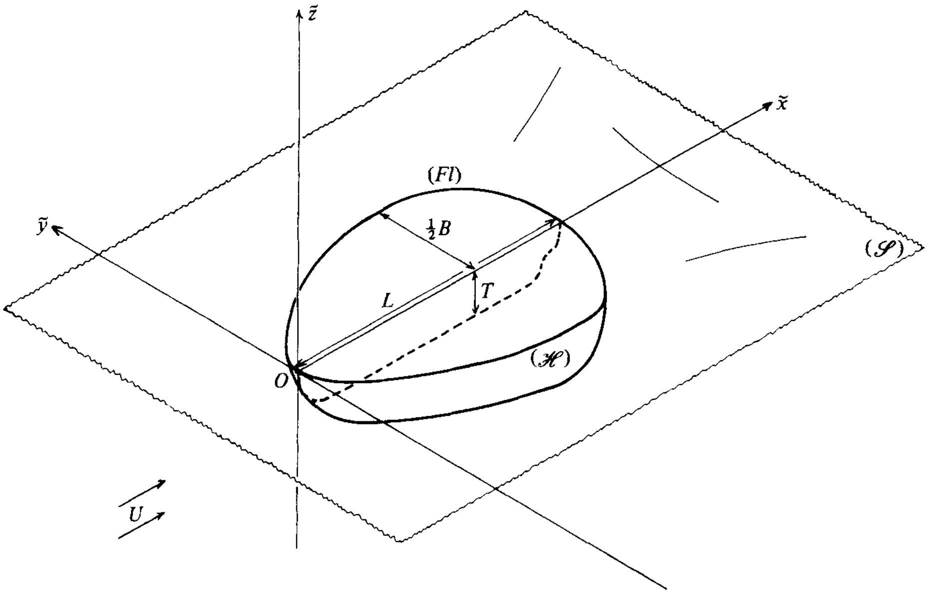

FIGURE 1. Dimensional configuration.
The dotted line represents the intersection between $\tilde{x}Oz$ and $(\mathscr{H})$.

computer; but, for the object of the present paper, it is sufficient to know the inner behaviour of its solution, which can be obtained directly with the aid of the variable-like method.

2. Statement of the problem

2.1. *Shape of the hull*

Let L, B, T be the length, beam and draft of the hull $(\mathscr{H})$ and g the gravity. The co-ordinate system $O\tilde{x}\tilde{y}\tilde{z}$ is fixed to the ship and defined such that (see figure 1):

(*a*) $O\tilde{x}\tilde{y}$ is the plane of the undisturbed free surface at infinity,

(*b*) $O\tilde{z}$ is the vertical upwards axis,

(*c*) O is the zero level point of the ship bow,

(*d*) $O\tilde{x}$ is parallel to the uniform incoming flow U, with $U > 0$.

The Froude number $F_L = U/(gL)^{\frac{1}{2}}$ is supposed to be of order unity. The shape of the ship is schematically characterized by two dimensionless parameters:

$$\epsilon = T/L, \quad b = B/L.$$

In order to apply the matched asymptotic expansions method, the ship will be considered as a small perturbation of the uniform flow in the following sense: b is not small compared to unity ($b \sim 1$), ϵ is much smaller than one ($\epsilon \ll 1$). The ship is thus a *flat ship*.

Let (Fl) be the intersection between the $O\tilde{x}\tilde{y}$ plane and the hull $(\mathscr{H})$. For the sake of computation simplicity, the precise shape of $(\mathscr{H})$ is the one depicted in figure 2, without dimensions (the tilde have been dropped). The features of this hull are as follows: (i) the bottom of the ship is flat; (ii) (Fl) has no sharp angle; (iii) the hull walls are generated by straight lines as indicated below.

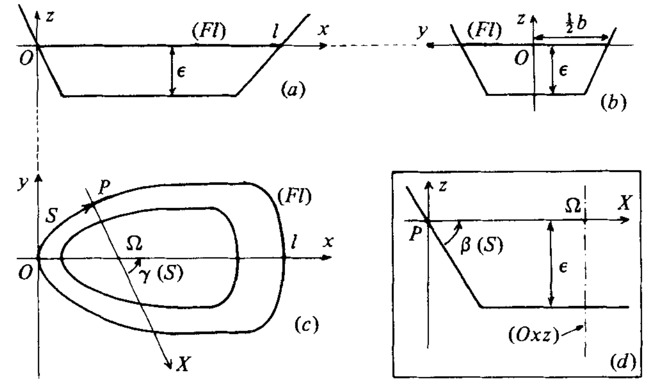

FIGURE 2. Non-dimensional definition of the hull: (a) side view; (b) front view; (c) view from top; (d) section of the ship in the XPz-plane.

Along (Fl), from O, is defined the curvilinear abscissa S, corresponding to the point P. Let PX be the inwards horizontal axis, normal to (Fl), and $\gamma(S)$ the angle between PX and Ox. The intersection between the wall and the vertical XPz plane is supposed to be rectilinear and to stand at a given angle $\beta(S)$ to the horizontal axis. It is meant by *blunt ship* that β is not small and remains constant as ϵ vanishes.

2.2 *Equations*

To study the vicinity of the walls, it is convenient to write down the equations of motion using the local co-ordinates (X, S, z). The non-dimensional unknowns are the velocity potential $\phi(X, S, z, \epsilon)$ and the free surface elevation $\eta(X, S, \epsilon)$. (These quantities are obtained by dividing the corresponding dimensional quantities respectively by UL and L.) The differential operators can be expressed in terms of (X, S, z); for instance, the velocity vector is

$$\nabla\phi = \left(\frac{\partial\phi}{\partial X} \quad \left[1-\frac{X}{R(S)}\right]^{-1}\frac{\partial\phi}{\partial S} \quad \frac{\partial\phi}{\partial z}\right),$$

where $R(S)$ is the local curvature radius of (Fl). A detailed analysis, given in Fernandez (1978), shows that ϕ and η satisfy the following criteria:

(i) ϕ is harmonic in the fluid domain D,

$$\phi_{XX}+\left(1-\frac{X}{R}\right)^{-2}\phi_{SS}+\phi_{zz}-\frac{1}{R}\left(1-\frac{X}{R}\right)^{-1}\phi_X-\frac{XR'}{R^2}\left(1-\frac{X}{R}\right)^{-3}\phi_S = 0, \tag{2.1}$$

where $R' = dR/dS$.

(ii) The fluid slips on the bottom of the ship,

$$\phi_z(X, S, -\epsilon) = 0, \quad 0 < X < X_\Omega, \tag{2.2}$$

(where X_Ω is the abscissa of the intersection Ω between PX and the xOz plane), and on the walls of the hull

$$\phi_X \sin\beta+\phi_z\cos\beta+\beta'\left(1-\frac{X}{R}\right)^{-2}(X\cos\beta-z\sin\beta)\,\phi_S = 0, \tag{2.3}$$

where $\beta' = d\beta/dS$.

(iii) The free surface $(\mathscr{S})$ is a stream surface,

$$\phi_z = \phi_X\eta_X+\left(1-\frac{X}{R}\right)^{-2}\phi_S\eta_S \quad \text{on} \quad (\mathscr{S}). \tag{2.4}$$

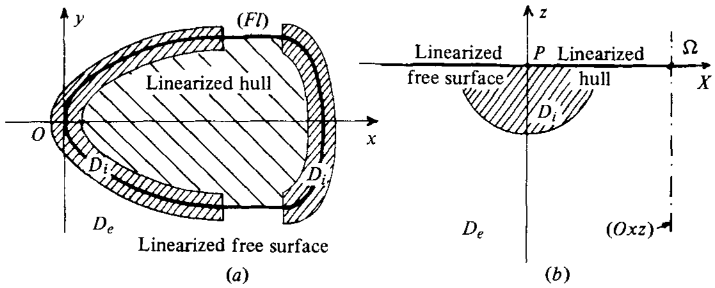

FIGURE 3. Inner domain D_i and outer domain D_e: (a) view from upside; (b) section by XPz.

(iv) The pressure distribution is continuous across the free surface,

$$\phi_x^2 + \left(1-\frac{X}{R}\right)^{-2} \phi_s^2 + \phi_z^2 + \frac{2}{F_L^2}\eta = K, \tag{2.5}$$

where K is constant.

(v) The uniform flow is not perturbed at infinity

$$X \to -\infty \left\{ \begin{array}{l} \phi - X\cos\gamma(S) - \int_0^s \sin\gamma(s)\,.\,ds \to 0, \\ \eta \to 0. \end{array} \right\} \tag{2.6}$$

3. Outer singular problem

The first step is to assume that the solution is expandable with respect to ϵ

$$\left. \begin{array}{l} \phi(X,S,z,\epsilon) = \phi_0(X,S,z) + \nu_1(\epsilon)\,\phi_1(X,S,z) + \nu_2(\epsilon)\,\phi_2(X,S,z) + \ldots, \\ \eta(X,S,\epsilon) = \eta_0(X,S) + \mu_1(\epsilon)\,\eta_1(X,S) + \mu_2(\epsilon)\,\eta_2(X,S) + \ldots, \end{array} \right\} \tag{3.1}$$

where $\nu_i(\epsilon)$ and $\mu_i(\epsilon)$ denote outer asymptotic sequences. When ϵ vanishes, the angle $\beta(S)$ being kept fixed, the hull shrinks to a body $(\mathscr{H}_0)$, the bottom of which is the part of the xOy plane bounded by (Fl). Bringing (3.1) into the complete equations (2.1)–(2.6) and letting $\epsilon \to 0$, one obtains the nonlinear problem of order zero. It is of interest to note that (2.3) is reduced to the condition

$$\phi_{0X}\sin\beta + \phi_{0z}\cos\beta + \beta'\left(1-\frac{X}{R}\right)^{-2}(X\cos\beta - z\sin\beta)\,\phi_{0S} = 0, \tag{3.2}$$

on the walls of $(\mathscr{H}_0)$. If the problem were regular, the order-zero problem would be satisfied by the undisturbed uniform flow, say

$$\phi_0 = X\cos\gamma(S) + \int_0^s \sin\gamma(s)\,.\,ds, \quad \eta_0 = 0. \tag{3.3}$$

It is easy to ascertain that all zeroth-order equations but (3.2) admit (3.3) as a solution. Indeed, if one introduces (3.3) into (3.2), one is lead to

$$\cos\gamma(S) = 0, \quad \text{i.e.} \quad \gamma(S) = \pm\tfrac{1}{2}\pi.$$

This establishes that the uniform flow may be accepted as the term of order zero in a linearized outer domain D_e, (Fl) being a singular line around which an inner domain

D_i must be defined, at least along the part which is not parallel to Ox (see figure 3). Hence starting from (2.1), (2.2), (2.4), (2.5), (2.6), (3.1), (3.3), it is a matter of simple algebra to compute the equations for successive outer orders, once the sequences ν_i, μ_i are known. Here lies a difficulty which must not be overlooked, as it will be seen below. The most secure way to find the outer sequences is to take up the outer expression of inner solution as a guide. Thus, it is convenient to state the inner problem.

4. Inner problem

The inner scale is the one which makes visible the hull geometry. More precisely, the inner variables are defined by

$$\bar{X} = \frac{X}{\epsilon}, \quad \bar{z} = \frac{z}{\epsilon}, \tag{4.1}$$

$$\bar{\eta}(\bar{X}, S, \epsilon) = \frac{1}{\epsilon}\eta(X, S, \epsilon), \quad \bar{\phi}(\bar{X}, S, \bar{z}, \epsilon) = \frac{1}{\epsilon}\phi(X, S, z, \epsilon). \tag{4.2}$$

Introducing these new variables into the full problem (2.1)–(2.5), one readily obtains the inner problem, the solution of which is looked for as a double expansion

$$\left.\begin{aligned} \bar{\phi}(\bar{X}, S, \bar{z}, \epsilon) &= \bar{\phi}_0(\bar{X}, S, \bar{z}) + \nu_1'(\epsilon)\,\bar{\phi}_1(\bar{X}, S, \bar{z}) + \dots, \\ \bar{\eta}(\bar{X}, S, \epsilon) &= \bar{\eta}_0(\bar{X}, S) + \mu_1'(\epsilon)\,\bar{\eta}_1(\bar{X}, S) + \dots . \end{aligned}\right\} \tag{4.3}$$

As a matter of fact, one will only look for the inner solution at order zero. Putting (4.3) into the complete inner problem, the equations at this order are easily derived; they may be written down

$$\bar{\phi}_{0\bar{z}} = \bar{\phi}_{0\bar{X}}\,\bar{\eta}_{0\bar{X}} \quad \text{on the free surface } (\mathscr{S}); \tag{4.4}$$

$$\bar{\phi}^2_{0\bar{X}} + \bar{\phi}^2_{0\bar{z}} = \omega_0^2 \quad \text{on the free surface } (\mathscr{S}); \tag{4.5}$$

$$\bar{\phi}_{0\bar{z}}\cos\beta + \bar{\phi}_{0\bar{X}}\sin\beta = 0 \quad \text{on the wall of the ship;} \tag{4.6}$$

$$\bar{\phi}_{0\bar{z}} = 0 \quad \text{on the bottom of the ship;} \tag{4.7}$$

$$\bar{\phi}_{0\bar{X}\bar{X}} + \bar{\phi}_{0\bar{z}\bar{z}} = 0 \quad \text{in the fluid domain.} \tag{4.8}$$

Here ω_0^2 denotes a positive constant.

In these equations, the curvilinear abscissa S appears only as a parameter; in the $\bar{X}P\bar{z}$-plane, this problem may be interpreted as the one of the two-dimensional motion of an ideal fluid without gravity, past an infinitely long two-dimensional body. This type of problem can be easily solved by conformal mapping.

5. Inner solution

In the method used so far, one does not assume anything about the free surface shape. It is now appropriate to consider different possibilities of contact between $(\mathscr{H})$ and $(\mathscr{S})$. One can *a priori* imagine three types† of flows (see figure 4).

(*a*) In the first type, the contact point C is a corner point. It is thus necessarily a stagnation point; hence $\omega_0 = 0$ and the fluid speed vanishes on the whole free surface.

† While this work was being reviewed, Vanden-Broeck (1980) has brought out a fourth type, with separation at the corner B of the ship. It is not yet established that this type lends itself to the same treatment as the others.

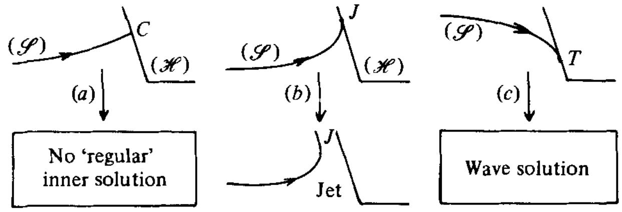

FIGURE 4. Inner solution: (a) corner; (b) upwards tangential contact; (c) downwards tangential contact.

In this case, it is however not possible to find an inner solution which is regular at finite distance and matches the outer solution. One may also look for a 'singular' inner solution, for instance using a second smaller inner zone. This direction has been followed without any success.

(b) The second type is an upward tangential contact. In the strict sense, it is the same case as above, except in the case where the contact point J is located at infinity. A jet rise thus occurs.

(c) The third type is a downward tangential contact which describes a wave formation.

With the help of conformal mapping, it is easy to establish that the two disclosed possibilities actually lead to two inner solutions. The calculations are too long to be detailed here and may be found in Fernandez (1978). Only the main results are given here.

5.1. *First inner solution: a jet*

Let $\bar{\zeta}$ be the complex variable $\bar{\zeta} = \bar{X} + i\bar{z}$ and q the inner jet thickness. The $\bar{\zeta}$ plane is mapped onto the auxiliary upper half t plane by

$$\frac{d\bar{\zeta}}{dt} = -\frac{q}{\pi}\left(\frac{1+\left(\frac{t-1}{t}\right)^{\frac{1}{2}}}{1-\left(\frac{t-1}{t}\right)^{\frac{1}{2}}}\right)^{\beta/\pi}\left(\frac{1-\frac{\beta}{\pi}\left(\frac{t-1}{t}\right)^{\frac{1}{2}}}{1+\frac{\beta}{\pi}\left(\frac{t-1}{t}\right)^{\frac{1}{2}}}\right)\frac{1+\left(\frac{\pi^2}{\beta^2}-1\right)t}{t(t-1)^2}. \tag{5.1}$$

The order zero of the inner solution may be given by the complex velocity

$$\bar{w}_0(t) = \omega_0\left(\frac{1+\left(\frac{t-1}{t}\right)^{\frac{1}{2}}}{1-\left(\frac{t-1}{t}\right)^{\frac{1}{2}}}\right)^{\beta/\pi}\left(\frac{1-\frac{\beta}{\pi}\left(\frac{t-1}{t}\right)^{\frac{1}{2}}}{1+\frac{\beta}{\pi}\left(\frac{t-1}{t}\right)^{\frac{1}{2}}}\right). \tag{5.2}$$

The corresponding flow is sketched in the figure 5.

Expanding that solution in the vicinity of $t = 1$, one may express the behaviour of the inner solution at infinity of the $\bar{\zeta}$ plane

$$\bar{\zeta}\to\infty, \quad \bar{w}_0 = \omega_0\left(1+\frac{2\pi A}{3}\left(\frac{q}{\bar{\zeta}}\right)^{\frac{3}{2}} - Aq^{\frac{3}{2}}\frac{\log\bar{\zeta}}{\bar{\zeta}^{\frac{3}{2}}} + B\left(\frac{q}{\bar{\zeta}}\right)^{\frac{3}{2}} + o\left[\frac{1}{\bar{\zeta}^{\frac{3}{2}}}\right]\right), \tag{5.3}$$

where $A = A(\beta/\pi)$ and $B = B(\beta/\pi, q)$ are constants, the expressions of which are given in appendix A.

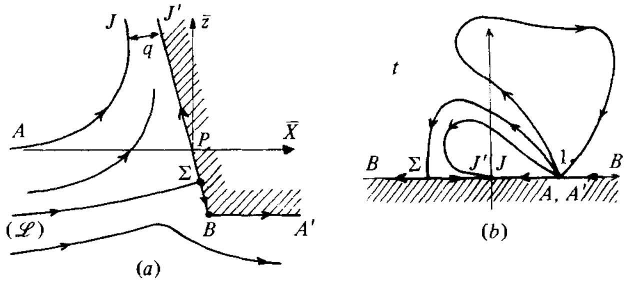

FIGURE 5. Jet flow in (a) the physical $\bar X P \bar z$-plane, (b) the auxiliary t-plane.

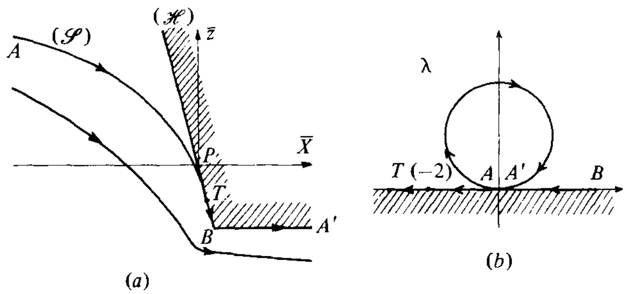

FIGURE 6. Wave flow in (a) the physical $\bar X P \bar z$-plane, (b) the auxiliary λ-plane.

5.2. *Second inner solution: a wave*

Similarly the physical plane is mapped onto an auxiliary upper half λ plane (see figure 6) by

$$\frac{d\bar\zeta}{d\lambda} = -\frac{c^2}{\lambda^2}\left(1+\lambda+[\lambda(\lambda+2)]^{\frac12}\right)^{-\beta/\pi}, \tag{5.4}$$

where c is a real constant related to the distance between the contact point T and the corner B, and the solution at the order zero is

$$\bar w_0(\lambda) = \omega_0[1+\lambda+(\lambda(\lambda+2))^{\frac12}]^{\beta/\pi}. \tag{5.5}$$

From (5.4) and (5.5), the behaviour of this solution at infinity can be obtained

$$\bar w_0 = \omega_0\left(1-\frac{\beta c}{\pi}\frac{\sqrt{2}}{\bar\zeta^{\frac12}}-\frac{\beta^2c^2}{\pi^2\bar\zeta}-\frac{\beta^3c^3\sqrt{2}}{2\pi^3}\frac{\log\bar\zeta}{\bar\zeta^{\frac32}}+A\frac{\beta c}{\pi\bar\zeta^{\frac32}}+O\left[\frac{\log\bar\zeta}{\bar\zeta^2}\right]\right), \tag{5.6}$$

where $A = A(\beta/\pi, c)$ is a constant given in appendix B.

At this stage, ω_0 and q in (5.3), as well as ω_0 and c in (5.6), are still unknown. They can be determined only from matching with the outer solution.

6. Outer solution

The outer expression of the inner solution indicates the appropriate outer sequence. For instance, setting $\bar\zeta = \zeta/\epsilon$ into (5.3) indicates that, besides the orders $1, \epsilon, \epsilon^2, \ldots$, orders of $\epsilon^{\frac32}, \epsilon^{\frac52}\log\epsilon$, etc., must be introduced. Thus for the jet solution the suitable sequence is

$$1, \epsilon, \epsilon^{\frac32}, \epsilon^2, \epsilon^{\frac52}\log\epsilon, \epsilon^{\frac52}, \ldots, \tag{6.1}$$

and for the wave solution it is

$$1, \epsilon^{\frac12}, \epsilon, \epsilon^{\frac32}\log\epsilon, \epsilon^{\frac32}, \ldots\,. \tag{6.2}$$

The jet case resolution only will be developed. The second solution can be dealt with quite similarly; the result only will be given.

The outer solution is taken as a double expansion

$$\phi(X,S,z,\epsilon) = \phi_0(X,S,z)+\epsilon\phi_1(X,S,z)+\epsilon^{\frac{3}{2}}R_1(X,S,z)+\epsilon^2\phi_2(X,S,z) + \epsilon^{\frac{5}{2}}\log\epsilon\, L_2(X,S,z)+\epsilon^{\frac{5}{2}}R_2(X,S,z)+\dots, \quad (6.3)$$

$$\eta(X,S,\epsilon) = \eta_0(X,S)+\epsilon\eta_1(X,S)+\epsilon^{\frac{3}{2}}H_1(X,S)+\epsilon^2\eta_2(X,S) + \epsilon^{\frac{5}{2}}\log\epsilon\Lambda_2(X,S)+\epsilon^{\frac{5}{2}}H_2(X,S)+\dots,$$

where
$$\phi_0 = X\cos\gamma(S)+\int_0^s \sin\gamma(s)\,ds, \quad \eta_0 = 0.$$

Substituting ϕ and η into the general equations and linearizing the conditions on both the free surface and the bottom of the ship, one obtains the problem for the successive outer orders. For instance, at ϵ order

$$\phi_{1XX}+\left(1-\frac{X}{R}\right)^{-2}\phi_{1SS}+\phi_{1zz}-\frac{1}{R}\left(1-\frac{X}{R}\right)^{-1}\phi_{1X}-\frac{XR'}{R^2}\left(1-\frac{X}{R}\right)^{-3}\phi_{1S} = 0, \quad z<0; \quad (6.4)$$

$$\phi_{1z}(X,S,0) = 0, \quad X\in\,]0,X_\Omega]; \quad (6.5)$$

$$\left.\begin{aligned}\phi_{1z} &= \eta_{1X}\cos\gamma+\left(1-\frac{X}{R}\right)^{-1}\eta_{1S}\sin\gamma \quad (6.6)\\ \eta_1 &= -F_L^2\left[\cos\gamma\phi_{1X}+\left(1-\frac{X}{R}\right)^{-1}\sin\gamma\,.\,\phi_{1S}\right] \quad (6.7)\end{aligned}\right\} \text{ on } (X,S,0),\quad X<0;$$

$$|\nabla\phi_1|\to 0, \quad \eta_1\to 0 \quad \text{at} \quad \infty. \quad (6.8)$$

This problem is but a special case of the Neumann–Kelvin problem, written using local curvilinear co-ordinates. The problems for the following orders are similar but more complicated as their order increases. It is not possible to solve these problems analytically. Nevertheless, we are interested only in knowing the local behaviour of their solutions in the vicinity of (*Fl*); and it is easy to obtain this behaviour thanks to the variable-like method: one introduces a 'small' arbitrary parameter δ (purely artificial and which may not be compared to ϵ) and one magnifies the *outer* variables by

$$X = \delta\hat{X}, \quad z = \delta\hat{z}, \quad (6.9)$$

directly in each *outer* problem. For instance, setting

$$\hat{\phi}_1(\hat{X},S,\hat{z},\delta) = \phi_1(\hat{X}\delta,S,\hat{z}\delta), \quad (6.10)$$

and inserting the new variables into the ϵ-order problem in which one eliminates η_1, one obtains

$$\hat{\phi}_{1\hat{X}\hat{X}}+\hat{\phi}_{1\hat{z}\hat{z}}-\frac{\delta}{R}\left(1-\delta\frac{\hat{X}}{R}\right)^{-1}\hat{\phi}_{1\hat{X}}+\delta^2\left(1-\delta\frac{\hat{X}}{R}\right)^{-2}\hat{\phi}_{1SS}-\delta^3\frac{\hat{X}R'}{R^2}\left(1-\delta\frac{\hat{X}}{R}\right)^{-3}\hat{\phi}_{1S} = 0, \quad \hat{z}=0; \quad (6.11)$$

$$\hat{\phi}_{1\hat{z}}(\hat{X},S,0,\delta) = 0, \quad \hat{X}>0; \quad (6.12)$$

$$\delta\hat{\phi}_{1\hat{z}}+F_L^2\left[\cos^2\gamma\,.\,\hat{\phi}_{1\hat{X}\hat{X}}+\delta\frac{\sin 2\gamma}{(1-\delta\hat{X}/R)}\hat{\phi}_{1S\hat{X}}-\frac{\delta}{R}\frac{\sin^2\gamma}{(1-\delta\hat{X}/R)}\hat{\phi}_{1\hat{X}}+\delta^2\frac{\sin^2\gamma}{(1-\delta\hat{X}/R)^2}\hat{\phi}_{1SS} + \frac{\delta^2}{R}\frac{\sin 2\gamma}{(1-\delta\hat{X}/R)^3}\left[1-\delta\hat{X}\frac{2\cos\gamma+R'\sin\gamma}{2R\cos\gamma}\right]\hat{\phi}_{1S}\right] = 0, \quad \hat{z}=0, \quad \hat{X}<0. \quad (6.13)$$

The conditions at infinity are lost when δ vanishes.

The solution of each outer order problem is then sought as an expansion† with respect to δ. The choice of the δ-sequence is guided by the knowledge of the outer behaviour of inner solution which indicates at the same time some terms of the δ-sequence and the degree of the outer singularity which one has to accept along (Fl). For example,

$$\hat{\phi}_1(\hat{X}, S, \hat{z}, \delta) = \delta^{\frac{1}{2}}\hat{\phi}_{10\cdot 5}(\hat{X}, S, \hat{z}) + \dots, \tag{6.14}$$

and the problem for the leading term $\hat{\phi}_{10\cdot 5}(\hat{X}, S, \hat{z})$, deduced from (6.11)–(6.14), is

$$\frac{\partial^2 \hat{\phi}_{10\cdot 5}}{\partial \hat{X}^2} + \frac{\partial^2 \hat{\phi}_{10\cdot 5}}{\partial \hat{z}^2} = 0, \quad \hat{z} < 0; \tag{6.15}$$

$$\frac{\partial \hat{\phi}_{10\cdot 5}}{\partial \hat{z}}(\hat{X}, S, 0) = 0, \quad \hat{X} > 0; \tag{6.16}$$

$$\frac{\partial^2 \hat{\phi}_{10\cdot 5}}{\partial \hat{X}^2}(\hat{X}, S, 0) = 0, \quad \hat{X} < 0. \tag{6.17}$$

These equations have a helpful characteristic: they are two-dimensional. Moreover, $\hat{\phi}_{10\cdot 5}$ is harmonic with respect to $(\hat{X}, \hat{z})$. They are thus easily solved using complex variables and the Hilbert method. Because these propitious circumstances occur for the leading terms of each outer order, one could say that the *problem* is locally two-dimensional. (It is worthwhile to emphasize that this does not imply that the outer *flow* itself is two-dimensional in the vicinity of (Fl). Indeed, the velocity is the vectorial sum of (i) a component $(0, [1 - X/R(S)]^{-1}\partial\phi/\partial S, 0)$ parallel to (Fl), (ii) a component $(\partial\phi/\partial X, 0, \partial\phi/\partial z)$ normal to (Fl); the preceding result means that, near the ship, the potential submits only to a weak dependence‡ on the co-ordinate S, so that the dependence on X and z of the latter component can be uncoupled.)

Then, to take into account that δ is an artificial parameter, one must impose that the δ-expansions contain $\delta, \hat{X}, \hat{z}$ only gathered into groups $(\delta\hat{X})$ and $(\delta\hat{z})$, which allows to come back to variables X and z.

As a result of the pseudo-two-dimensional character of the outer solution, the result may be given in terms of complex variables in the XPz-plane using $\zeta = X + iz$

$$\begin{aligned} w = {} & \cos\gamma(S) + \epsilon\left\{\frac{k_0(S)}{\zeta^{\frac{1}{2}}} + o(1)\right\} + \epsilon^{\frac{3}{2}}\left\{\frac{k_1(S)}{\zeta^{\frac{3}{2}}} + o\left(\frac{1}{\zeta}\right)\right\} \\ & + \epsilon^2\left\{-\frac{k_0(S)}{2\pi\zeta^{\frac{3}{2}}}[\log\zeta + k_3(S) - i\pi] + o\left(\frac{1}{\zeta^{\frac{3}{2}}}\right)\right\} + \epsilon^{\frac{5}{2}}\log\epsilon\left\{\frac{k_2(S)}{\zeta^{\frac{5}{2}}} + o\left(\frac{1}{\zeta^2}\right)\right\} \\ & + \epsilon^{\frac{5}{2}}\left\{-\frac{3k_1(S)}{2\pi\zeta^{\frac{5}{2}}}[\log\zeta + k_4(S) - i\pi] + o\left(\frac{1}{\zeta^{\frac{5}{2}}}\right)\right\} + o(\epsilon^{\frac{5}{2}}). \end{aligned} \tag{6.18}$$

† Note that the δ-expansion is not an asymptotic expansion in the sense of the matched asymptotic expansions technique, but only an expression showing the leading terms of the δ-expanded function in the vicinity of (Fl).

‡ This situation is similar to that occurring in the slender-ship theory in which the outer three-dimensional flow behaves two-dimensionally near the ship, despite the longitudinal flow (see Tuck 1964).

In the case of the wave solution, the same method leads to

$$w = \cos\gamma(S) + \epsilon^{\frac{1}{2}}\left\{\frac{K_0(S)}{\zeta^{\frac{1}{2}}} + o(1)\right\} + \epsilon\left\{-\frac{K_0^2(S)}{2\zeta} + o\left(\frac{1}{\zeta}\right)\right\} + \epsilon^{\frac{3}{2}}\log\epsilon\left\{\frac{K_1(S)}{\zeta^{\frac{3}{2}}} + o\left(\frac{1}{\zeta}\right)\right\}$$
$$+\epsilon^{\frac{3}{2}}\left\{-\frac{K_0(S)}{2\pi}[1+K_2(S)]\frac{\log\zeta}{\zeta^{\frac{3}{2}}} - \frac{K_0(S)}{2\pi}([1+K_2(S)]\,K_3(S) - i\pi[1+2K_2(S)])\right.$$
$$\left.\times\frac{1}{\zeta^{\frac{3}{2}}} + o\left(\frac{1}{\zeta^{\frac{3}{2}}}\right)\right\} + o(\epsilon^{\frac{3}{2}}). \tag{6.19}$$

In both cases, the real 'constants' $k_i(S), K_i(S)$ are not yet determined.

7. Matching of the outer and inner solutions

When expressed with the inner variable $\bar{\zeta} = \zeta/\epsilon$, the preceding results (6.18) and (6.19) give the inner behaviour of the outer solutions.

7.1. *Jet solution*

One obtains

$$w(\zeta) = \log\epsilon\,.\left\{\frac{k_2(S) - \dfrac{3k_1(S)}{2\pi}}{\bar{\zeta}^{\frac{5}{2}}}\right\} + \cos\gamma(S) + \frac{k_1(S)}{\bar{\zeta}^{\frac{3}{2}}} - \frac{3k_1(S)}{2\pi\bar{\zeta}^{\frac{5}{2}}}[\log\bar{\zeta} + k_4(S) - i\pi] + \dots\,. \tag{7.1}$$

In order to match (7.1) with (5.3), one must first eliminate the $\log\epsilon$-term

$$k_2(S) = \frac{3k_1(S)}{2\pi}. \tag{7.2}$$

Then

$$\omega_0 = \cos\gamma(S), \tag{7.3}$$

$$\omega_0\frac{2\pi A}{3}q^{\frac{3}{2}} = k_1(S), \tag{7.4}$$

$$\omega_0 A q^{\frac{5}{2}} = \frac{3k_1(S)}{2\pi}, \tag{7.5}$$

$$\omega_0 B q^{\frac{5}{2}} = -\frac{3k_1(S)}{2\pi}[k_4(S) - i\pi]. \tag{7.6}$$

Therefore matching is possible; equation (7.3) gives ω_0; equations (7.4) and (7.5) imply $q = 1$. Hence the matching determines completely the inner-order zero. As a consequence, the jet rate of flow d is known

$$d = \epsilon\,.\cos\gamma(S). \tag{7.7}$$

7.2. *Wave solution*

The inner expression of (6.19) is

$$w = \log\epsilon\left\{\frac{K_1(S) - \dfrac{K_0(S)}{2\pi}[1+K_2(S)]}{\bar{\zeta}^{\frac{3}{2}}}\right\} + \cos\gamma(S) + \frac{K_0(S)}{\bar{\zeta}^{\frac{1}{2}}} - \frac{K_0^2(S)}{2\bar{\zeta}}$$
$$-\frac{K_0(S)}{2\pi}[1+K_2(S)]\frac{\log\bar{\zeta}}{\bar{\zeta}^{\frac{3}{2}}} - \frac{K_0(S)}{2\pi}([1+K_2(S)]\,K_3(S) - i\pi[1+2K_2(S)])\frac{1}{\bar{\zeta}^{\frac{3}{2}}} + \dots\,. \tag{7.8}$$

In order to match it with (5.6) the $\log \epsilon$-term must vanish

$$K_1(S) = \frac{K_0(S)}{2\pi}[1+K_2(S)], \tag{7.9}$$

and

$$\omega_0 = \cos\gamma(S), \tag{7.10}$$

$$-\omega_0 c\frac{\beta}{\pi}\sqrt{2} = K_0(S), \tag{7.11}$$

$$-\omega_0\frac{\beta^2}{\pi^2}c^2 = -\frac{K_0^2(S)}{2}, \tag{7.12}$$

$$\omega_0\frac{\beta^3}{\pi^3}c^3\frac{\sqrt{2}}{2} = \frac{K_0(S)}{2\pi}[1+K_2(S]), \tag{7.13}$$

$$\omega_0 A\frac{Bc\sqrt{2}}{\pi} = -\frac{K_0(S)}{2\pi}([1+K_2(S)]K_3(S)-i\pi[1+2K_2(S)], \tag{7.14}$$

once again, matching is possible; equation (7.10) gives ω_0. But, in the present case, it must be emphasized that the inner-order zero is *not* determined thoroughly (one constant is still unknown, say c). This is because this inner solution describes the birth of a wave, the length of which is large compared with the inner scale ϵ; the crest of the wave is thus out of the inner zone – and out of the local outer δ zone – and the wave height (related to c, for instance) remains unknown. The full determination of the wave solution would require a complete numerical computation of the outer flow.

7.3. *Discussion and experimental verification*

Summarizing the results obtained so far, it is established that, at a given position S along (Fl), two solutions are possible. In order to distinguish between them, one can first easily show that, if one of these solutions is accepted at a certain abscissa S of the fore section (respectively, of the aft section) of the ship, it must be accepted necessarily on the whole fore section (respectively aft section) up to the point where (Fl) is parallel to Ox; this is to save the continuity of the representation. Then, one may notice the following

(*a*) The jet is not acceptable in the vicinity of the stern, and ideal fluid solutions with waves upstream must be refused.

(*b*) The horizontal pressure forces, integrated vertically along the wall of the ship are directed inwards for the jet solution, and outwards for the wave solution. Their contribution to the wave resistance is thus positive only if the jet is before the ship and the wave behind her. Hence, along the forepart of (Fl), the flow is described by the jet model while, along the aft section, the wave model is convenient (see figure 7). Particularly, in the vicinity of the bow, one obtains the description of a sheet of water which rises with a maximum intensity at the nose of the ship and fades out as the angle between Ox and (Fl) decreases. In addition, the sheet of water is formed in the inner zone, but its evolution occurs at outer scale, and it falls down again far enough to neglect re-entry jet.

In order to verify these results, a short test has been performed in the Bassin d'Essais des Carènes de Paris; a typical run is shown in the figure 8 (*a*).

At the stern, the presence of a viscous wake makes the interpretation of the visual observations difficult. However, it is clear that, for large enough F_L, the above wave

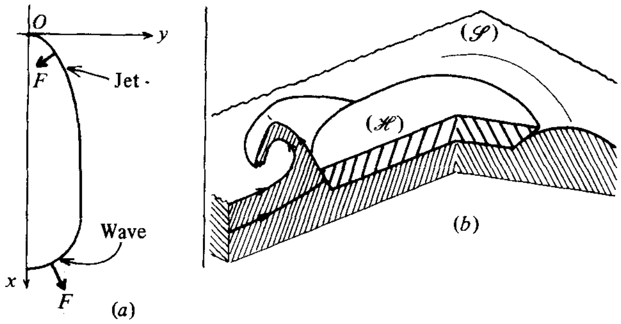

FIGURE 7. Three-dimensional flow past a flat blunt ship: (*a*) view from upside with horizontal pressure forces distribution F; (*b*) perspective view, with two sections, showing the sheet of water fading out along the fore part of the ship and the wave along the rear part.

solution does not occur. This indicates that this solution is not stable. The real flow would be better described with the aid of the solution of Vanden-Broeck (1980).

On the contrary, at the bow, the agreement with the jet solution is good enough. The rise of the sheet of water is observed (see figure 8*b*). Figure 9 presents the experimental decrease of the jet height along the water line compared with the one predicted from the present model. At the bow ($\gamma \simeq 0$), the jet height is overestimated by the theory because the viscous effects are neglected; while for greater γ, the jet height is underestimated owing to three-dimensional effects corresponding to orders higher than the one considered in the above-mentioned expansions. Nevertheless, on the whole, the theoretical prediction is satisfying.

8. Discrepancy with the results of I concerning high Froude number

The same method has been applied to the two-dimensional case of a blunt ship, the draft of which is ϵ, and has led to similar results featured in figure 10. At the stern, one obtains a wave. At the bow, the convenient solution is a two-dimensional jet; its thickness is determined from matching and is $t = \epsilon$.

With the same notation, it was found in I that t was of order ϵ^2. This discrepancy may indicate a possible mistake in those results. In order to support this opinion, it is worthwhile to make three remarks.

(*a*) The jet thickness expressed in I using inner variables is $\tilde{t}$ of order ϵ. This result introduces ϵ in the zero-order of their inner solution. From the mathematical point of view of the matched asymptotic expansions method, this is not correct because the order zero is not supposed to depend on ϵ.

(*b*) Moreover, the order zero in the inner solution represents a flow without gravity. Now $\epsilon = gTU^{-2}$. Hence, gravity is reintroduced into the equations of a flow without gravity through the small parameter; which seems to be a contradiction.

(*c*) Lastly, if M is a point at the free surface defined in their auxiliary plane $\tilde{\zeta}$ (see figure 11) by

$$\tilde{\zeta}_M = -\tilde{\rho} + i0^-, \quad \tilde{\rho} > 0. \tag{8.1}$$

Starting from their formula (37), p. 536, it is easy to compute the vertical co-ordinate of M, when $\tilde{\rho} \to +\infty$

$$\tilde{y}(M) = -\frac{2a\epsilon^{\frac{1}{2}}}{\pi^{\frac{1}{2}}}\tilde{\rho}^{\frac{1}{2}} + \left[\frac{a^2\epsilon}{4} - 1\right] + o(1). \tag{8.2}$$

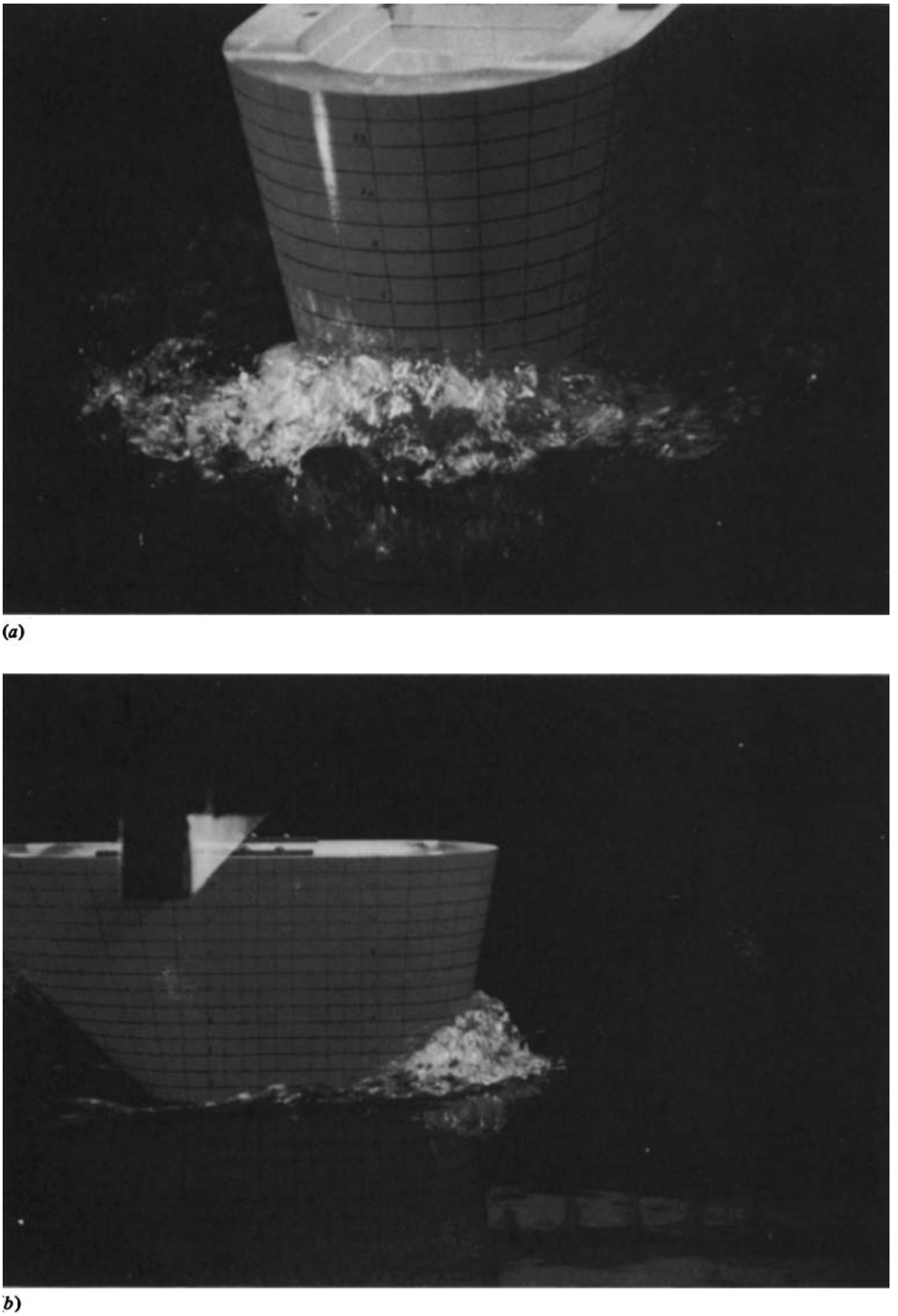

(a)

(b)

FIGURE 8. Model test at the Bassin d'Essais des Carènes de Paris: $L = 0{\cdot}4$ m, $B = 0{\cdot}2$ m, $T = 0{\cdot}02$ m; so that: $b = 0{\cdot}5$, $\epsilon = 0{\cdot}05$. Along the fore part and the walls, $\beta(S) = \text{const.} = 80°$. (Fl) is the water line number 0. The towing speed is $U = 1{\cdot}5 \text{ m s}^{-1}$, hence $F_L = 0{\cdot}76$. (a) front view, (b) side view.

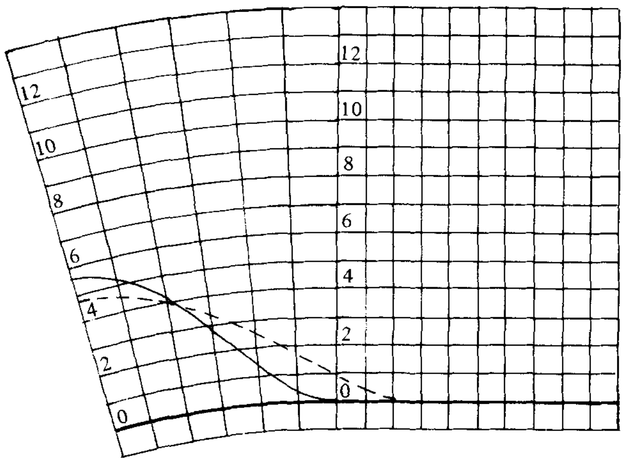

FIGURE 9. Cylindrical projection of the wave-top profile onto the body hull: – – –, experimental; ——, theoretical (the hull is developed).

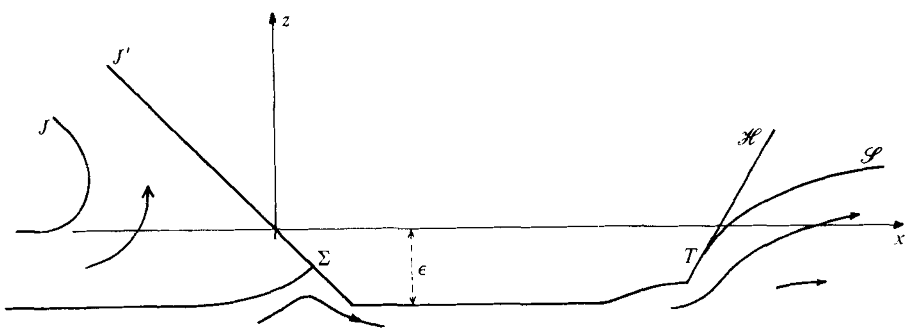

FIGURE 10. Two-dimensional flow past a flat blunt ship.

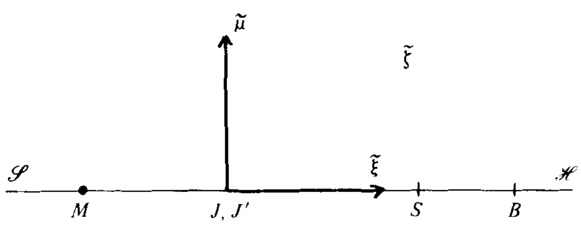

FIGURE 11. After figure 6(*c*) of I; *M* is a point running on the free surface.

This means that, in front of the ship, in inner zone, there is a free surface depression which is deeper than the ship draft. So this solution seems physically unacceptable.

The same difficulties were met by the author of the present paper; they were shown to point out an *incomplete* outer asymptotic sequence. As a matter of fact, to make the solution in I correct, $\tilde{l}$ must be of order unity in their formula (69), p. 541; then (70) shows that the outer sequence must be completed by a term $\epsilon^{\frac{1}{2}}$.

9. Conclusion

The main features of this paper are the following two assumptions: first, the body shape is somewhat rough-hewn in order to allow an analytical study of the flow, but the main characteristic which has to be emphasized is the bluntness; secondly, the square Froude number is of order one. For the present theory, the latter assumption is essential. As a consequence of it, the problem can be treated by dividing the fluid domain into two parts

(*a*) an 'outer' domain, the size of which is of the same order of magnitude as the body length. In this region, the free-surface condition is of the Kelvin type. On the contrary, if U^2/g were small compared with L, $F_L^2\phi_{xx}$ would be small compared with ϕ_z in equation (1.1) and, therefore, the leading term of ϕ would rather satisfy a free-surface condition of the Neumann type. This would make more suitable a model such as the slow-ship theory of Baba & Hara (1977).

(*b*) an 'inner' domain, small compared with the ship length, but which cannot be neglected. In this region, the nonlinearities dominate.

This situation has first a practical consequence for the numerical study of the subject: it is probably not useful to solve the complete nonlinear problem in the whole flow domain, as do Tuck & Vanden-Broeck. It is undoubtedly possible and sufficient to treat a twofold problem: linear far from the body and nonlinear only near the body.

It has also a more general consequence: when one uses the Neumann–Kelvin model to compute the flow past a blunt ship (i) whether the two terms of equation (1.1) are of the same order of magnitude ($F_L^2 \sim 1$), then the model is not valid, except if one takes into account the nonlinearities in the vicinity of the ship, (ii) or they are of different orders of magnitude ($F_L^2 \ll 1$), then the model is not really consistent but, nevertheless, the computation may happen to be practically efficient, at least within a certain range of F_L^2 values. In this case, the question is: what is the limit?

This work is based on the author's I.D. thesis (University Pierre et Marie Curie, 1978) which has been supported by the Ministère de la Défense.

Appendix A. Expression of A and B in (5.3)

The computation of A and B is not really difficult, but is too long to be given here. The result is

$$A = \frac{1-(\beta/\pi)^2}{\beta^2\pi^{\frac{1}{2}}},$$

$$B = \pi^2\frac{1-(\beta/\pi)^2}{5\beta^4\pi^{\frac{1}{2}}}\left\{2\left(\frac{\beta}{\pi}\right)^2 - 3 - 5X_0 + 5i\frac{\beta^2}{\pi q} - 5\frac{\beta^2}{\pi^2}\log\left(\frac{\beta^2}{\pi q}\right)\right\},$$

where
$$X_0 = -1 + \frac{\beta^2}{\pi}\cot g\beta + \int_0^1 G(x)\,dx + \int_1^{+\infty}\left[G(x) - 1 + \frac{\beta^2}{\pi^2 x}\right]dx$$

using
$$G(x) = \left(\frac{(x+1)^{\frac{1}{2}}-1}{(x+1)^{\frac{1}{2}}+1}\right)^{\beta/\pi}\left(\frac{(x+1)^{\frac{1}{2}}+\dfrac{\beta}{\pi}}{(x+1)^{\frac{1}{2}}-\dfrac{\beta}{\pi}}\right)\left[1-\frac{(\beta/\pi)^2}{x+1}\right].$$

Appendix B. Expression of A in (5.6)

Similarly to the above:

$$A = \left(\frac{\beta}{\pi}\right)^2 c^2\sqrt{2}\,[1+\log c] - \frac{c^2\sqrt{2}}{12}\left[4\left(\frac{\beta}{\pi}\right)^2 - 1\right] - \frac{\bar{x}_0}{\sqrt{2}} + i\pi\left[\left(\frac{\beta c}{\pi}\right)^2 + \frac{1}{2\pi}\right]\sqrt{2},$$

where

$$\bar{x}_0 = \frac{1}{tg\beta} + c^2\left\{2\sqrt{2}\left(\frac{\beta}{\pi}\right) - 1 + \int_0^1 \left(\frac{x}{1+x+(1+2x)^{\frac{1}{2}}}\right)^{\beta/\pi} dx + \int_1^{+\infty}\left[\left(\frac{x}{1+x+(1+2x)^{\frac{1}{2}}}\right)^{\beta/\pi} - 1 + \frac{\beta\sqrt{2}}{\pi x^{\frac{1}{2}}} - \frac{\beta^2}{\pi^2 x}\right] dx\right\}.$$

REFERENCES

BABA, E. & HARA, M. 1977 Numerical evaluation of a wave-resistance theory for slow ships. *Proc. 2nd Int. Conf. Num. Ship Hydrodynamics*, pp. 17–29.

BRARD, R. 1972 The representation of a given ship form by singularity distributions when the boundary condition on the free surface is linearized. *J. Ship Res.* **16**, 79–92.

CHANG, M. S. 1977 Computations of three-dimensional ship-motions with forward speed. *Proc. 2nd Int. Conf. Num. Ship Hydrodynamics*, pp. 124–135.

DAGAN, G. & TULIN, M. P. 1972 Two-dimensional free surface gravity flow past blunt bodies. *J. Fluid Mech.* **51**, 529–543.

FERNANDEZ, G. 1978 Etude de la non-linéarité de l'interaction carène-surface libre pour un navire avançant à vitesse uniforme en eau calme. *Rapport E.N.S.T.A.* no. 100. Paris.

GUÉVEL, P., DELHOMMEAU, G. & CORDONNIER, J. P. 1977 Numerical solution of the Neumann–Kelvin problem by the method of singularities. *Proc. 2nd Int. Conf. Num. Ship Hydrodynamics*, pp. 107–123.

JAMI, A. & LENOIR, M. 1978 A variational formulation for exterior problems in hydrodynamics. *Comp. Math. Appl. Mech. Engng* **16**, 341–359.

NEWMAN, J. N. 1976 Linearized wave resistance theory. *Int. Sem. Wave Resistance, Japan*, pp. 31–43.

NGUYEN, N. T. & ROJDESTVENSKII, K. 1975 Hydroplanage d'une plaque plane de grande envergure sur la surface d'un domaine fluide de profondeur finie. *J. Méc.* **14**, 793–821.

NICHOLS, B. D. & HIRT, C. W. 1975 Methods for calculating multi-dimensional, transient, free surface flows past bodies. *Proc. 1st Int. Conf. Num. Ship Hydrodynamics*, pp. 253–277.

NOBLESSE, F. 1976 What is the proper linear model and perturbation scheme for the flow around a ship? *Int. Sem. Wave Resistance, Japan*, pp. 393–398.

TUCK, E. O. 1964 A systematic asymptotic expansion procedure for slender ships. *J. Ship Res.* **8**, 15–23.

TUCK, E. O. 1977 Invited discussion. *Proc. 2nd Int. Conf. Num. Ship Hydrodynamics*, pp. 104–105.

TUCK, E. O. & VANDEN-BROECK, J.-M. 1977 Computation of near-bow or stern flows, using series expansions in the Froude number. *Proc. 2nd Int. Conf. Num. Ship Hydrodynamics*, pp. 371–381.

VANDEN-BROECK, J.-M. 1980 Nonlinear stern waves. *J. Fluid Mech.* **96**, 603–611.